The Journal of Experimental Biology 211, 686-698
Published by The Company of Biologists 2008
doi:10.1242/jeb.013938

The sound field generated by tethered stingless bees (*Melipona scutellaris*): inferences on its potential as a recruitment mechanism inside the hive

Michael Hrncir[1,2,*], Dirk Louis P. Schorkopf[2], Veronika M. Schmidt[2], Ronaldo Zucchi[1] and Friedrich G. Barth[2]

[1]Department of Biology, University of São Paulo, FFCLRP, Av. Bandeirantes 3900, 14040-901 Ribeirão Preto, SP, Brazil and
[2]Department of Neurobiology and Cognition Research, University of Vienna, Althanstrasse 14, A-1090 Vienna, Austria

*Author for correspondence (e-mail: michael.hrncir@gmx.at)

Accepted 17 December 2007

SUMMARY

In stingless bees, recruitment of hive bees to food sources involves thoracic vibrations by foragers during trophallaxis. The temporal pattern of these vibrations correlates with the sugar concentration of the collected food. One possible pathway for transfering such information to nestmates is through airborne sound. In the present study, we investigated the transformation of thoracic vibrations into air particle velocity, sound pressure, and jet airflows in the stingless bee *Melipona scutellaris*. Whereas particle velocity and sound pressure were found all around and above vibrating individuals, there was no evidence for a jet airflow as with honey bees. The largest particle velocities were measured 5 mm above the wings (16.0±4.8 mm s^{-1}). Around a vibrating individual, we found maximum particle velocities of 8.6±3.0 mm s^{-1} (horizontal particle velocity) in front of the bee's head and of 6.0±2.1 mm s^{-1} (vertical particle velocity) behind its wings. Wing oscillations, which are mainly responsible for air particle movements in honey bees, significantly contributed to vertically oriented particle oscillations only close to the abdomen in *M. scutellaris* (distances ⩽5 mm). Almost 80% of the hive bees attending trophallactic food transfers stayed within a range of 5 mm from the vibrating foragers. It remains to be shown, however, whether air particle velocity alone is strong enough to be detected by Johnston's organ of the bee antenna. Taking the physiological properties of the honey bee's Johnston's organ as the reference, *M. scutellaris* hive bees are able to detect the forager vibrations through particle movements at distances of up to 2 cm.

Key words: stingless bees, thorax vibration, airborne sound, airflow, particle velocity, signal transmission, recruitment communication.

INTRODUCTION

In the analysis of communication systems, knowledge of the physical nature of the signals transmitted is of fundamental importance and represents an important step towards the identification of potential receivers. When collecting at highly profitable nectar sources, stingless bee foragers of the genus *Melipona* generate pulsed thorax vibrations upon their return to the nest. In all cases studied so far, the temporal pattern of these vibrations predominantly and highly significantly correlated with the sugar concentration of the collected food (Hrncir et al., 2006a). There are three potential pathways for the transmission of this information to prospective recruits: (i) direct contact during trophallaxis (Hrncir et al., 2006b), (ii) substrate vibrations (Lindauer and Kerr, 1958), and (iii) airborne sounds (Esch, 1967; Nieh, 1998; Nieh et al., 2003). So far, only pathways (i) and (ii) have been investigated in some detail in *Melipona* bees (Hrncir et al., 2000; Hrncir et al., 2006b; Hrncir, 2003; Morawetz, 2007; Morawetz et al., 2007).

Current knowledge of the transformation of thoracic vibrations to airborne sound is based on a few studies in honey bees (Esch, 1961; Wenner, 1962; Michelsen et al., 1986; Michelsen et al., 1987; Michelsen, 2003) and in bumble bees (Schneider, 1975). In honey bees, wing oscillations going along with the thoracic vibrations transform these into airborne sound (Esch, 1961; Wenner, 1962; Michelsen et al., 1987). In bumble bees, on the other hand, wing oscillations are not significantly involved in the emission of airborne sound (Schneider, 1975). The defence sounds of bumble bee queens (sound pressure), which could be recorded behind, laterally and in front of the bees, remained largely unaffected by the partial or even the complete ablation of the wings (Schneider, 1975).

The physical parameter of airborne sound relevant as input to Johnston's organ in the pedicellus of the bees' antenna, the mechanoreceptor potentially involved in its perception, is air particle movement (Dreller and Kirchner, 1993; Michelsen, 1993). Close to the abdomen of dancing honey bees, strong air particle oscillations with velocity amplitudes of up to 70 cm s^{-1} (peak to peak, p-p) were measured. This value decreased rapidly with distance from the bee (Michelsen et al., 1987). In addition to these particle oscillations, honeybees generate a unidirectional 'jet airflow' during their dance, but only when the wingtips of the dancer are apart by more than 7 mm (Michelsen, 2003). The study of a mechanical bee model suggested that this airflow, directed away from the abdomen, is formed by the air emanating from the space between the wings and the abdomen. In contrast to the air particle oscillations, the amplitude of the jet airflow decreased only slowly and linearly with distance to the bee (Michelsen, 2003).

In stingless bees, nothing is known so far about the transformation of thoracic vibrations to airborne sound, even though airborne sound has been considered important as a carrier of information (Esch, 1967; Nieh, 1998; Nieh et al., 2003). In the present study, we therefore asked the following questions. (1) How strong is the airborne sound (particle velocity and sound pressure) generated by vibrating stingless bees? (2) Is airborne sound limited to the abdominal region of the vibrating bee, as is the case in honey bees? (3) How important are the wings for the transformation of thorax

vibrations to airborne sound? (4) Do vibrating stingless bees generate 'jet airflows' like honey bees? (5) Do hive bees stay close enough to a forager to detect with their antennae the particle velocity resulting from the forager's thoracic vibrations?

MATERIALS AND METHODS

Bees and study site

Stingless bees *Melipona seminigra* Friese 1903 generate pulsed 'annoyance buzzing' when tethered with a sling around their neck (Hrncir et al., 2008). Although annoyance buzzing differed significantly with respect to both the main frequency component and the velocity amplitude from forager vibrations, the mechanism of generation is similar in these two types of vibrations. Most importantly for their putative transformation into airborne sounds (Michelsen et al., 1987), both vibration types resulted in oscillations of the wings to a similar degree (average velocity amplitude measured at the wingtips: annoyance buzzing, 688 mm s^{-1}; forager vibrations, 660 mm s^{-1}; average gain between thorax and wingtips: annoyance buzzing, 16.2 dB; forager vibrations, 17.9 dB) (Hrncir et al., 2008). The way that thoracic vibrations are transformed into airborne sounds, therefore, is very similar in these two types of vibrations. The study of annoyance buzzing has the great advantage over the study of forager vibrations that the first type of vibrations is generated in a controllable environment and sensors can be easily positioned around the bees. However, differences in the absolute values of particle velocity and sound pressure due to differences in the velocity amplitude and the main frequency component between the two vibration types must be taken into account.

In the present study we examined bees of the species *Melipona scutellaris* Latreille 1811, which are similar in size to *M. seminigra*, and reliably emit annoyance buzzing when sling-tethered as well (M.H., unpublished). Two colonies were housed in wooden nest-boxes inside a laboratory building on the campus of the University of São Paulo in Ribeirão Preto, Brazil. For video recordings of trophallactic interactions between foragers and hive bees we installed an acrylic, glass-covered observation box (10×5×4 cm^3) between the nest and the entrance/exit tube through the wall. In most of the cases the returning foragers distributed their nectar or sugar water among nestmates inside this observation box (see Hrncir et al., 2004b; Hrncir et al., 2006b). The recordings described in the present study were made between December 2005 and April 2006.

Sound field generated by vibrating bees

We measured the air particle velocity (amplitude p-p) and the sound pressure (pressure amplitude p-p) induced by the thoracic vibrations of sling-tethered bees. Sound pressure is not of immediate importance here because no pressure receivers are known in bees. Yet, sound pressure measurements enabled us to compare our results with those of the existing literature. Both air particle velocity and sound pressure were recorded using a Microflown^{TM} USP-probe (UT0406-5, Microflown Technologies, Arnhem, The Netherlands) which combines three particle velocity sensors (sensitivity: 15 mV/[mm s^{-1}]) and a pressure microphone (sensitivity: 14 mV/Pa). At frequencies relevant for the present study [main frequency range of stingless bee thorax vibrations: 200–600 Hz (Hrncir et al., 2006a)], particle velocities measured with the USP-probe showed an average deviation of 12.7% (range: 8–18%) from particle velocities measured under the same experimental conditions in our Vienna laboratory by means of particle image velocimetry (DPIV system: 2 New wave Mercury Nd:YAG lasers and an IDT iNanoSense TR camera, Dantec Dynamics, Skorlunde, Denmark). Hence, an average measurement error of ±1.07 dB relative to the DPIV measurements has to be taken into consideration for the particle velocities recorded in the present study.

To record the sound field around sling-tethered individuals (N_{total}=47), bees were placed on a plane acrylic substrate (15×15 cm^2). Particle velocity was measured both above and around the vibrating bees (Fig. 1). The sensor positions were at distances of 5, 10, 15 and 20 mm from the bee (Fig. 1). Due to slight, inevitable movements of the bees during the recordings, the accuracy of these measurement distances was ±1 mm. Above the bees (N=11), we measured the particle velocity oriented perpendicularly to the substrate above the head, above the thorax and above the wings close to the wingtips (Fig. 1B, inset). In the plane around the bee (5 mm above the substrate), two components of particle velocity were investigated: (i) the particle velocity oriented perpendicularly to the substrate (vertically oriented particle velocity; N=12), and (ii) the particle velocity oriented parallel to the substrate and towards/away from the vibrating bee (horizontally oriented particle velocity, N=12) (ii) (Fig. 1). In addition to the particle velocity caused by the vibrating bee itself, part of the vertically oriented particle velocity originated from

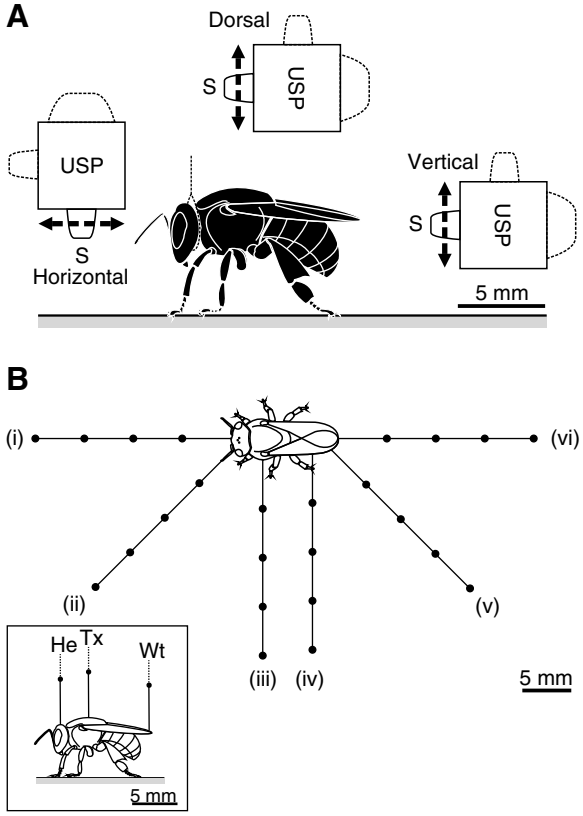

Fig. 1. Airborne sound (sound pressure, mPa, and air particle velocity, mm s^{-1}) generated by sling-tethered stingless bees was measured using a Microflown^{TM} USP-probe. (A) We measured particle velocity in the horizontal plane around the bee as well as above the vibrating individual. In the horizontal plane, the microphone to measure sound pressure and the airflow sensors (S) to measure air particle velocity either parallel to the substrate or perpendicular to it were kept at a constant distance of 5 mm above the plane acrylic plate used as substrate (15×15 cm^2). (B) Sound pressure and air particle velocity were picked up at 24 different measurement points in the horizontal plane around the vibrating bee. The different directions of the measurement points relative to the long axis of the bee were labelled (i-vi). Inset: USP probe positions above the bee's head (He), thorax (Tx) and wingtips (Wt); only measurement points (filled circles) at 5 mm distance are shown.

sound reflected by the substrate. During foraging, collecting bees generate their thoracic vibrations predominantly close to the nest entrance on particular structures made of stiff batumen (Hrncir et al., 2006b; Morawetz, 2007; Morawetz et al., 2007). These often tubular 'entrance structures' certainly also reflect the airborne sounds produced by foragers. Due to the irregular form of the entrance structures, however, and due to the variability in the materials used, sound reflections in the natural situation are expected to be more complex than those from the flat acrylic surface used in the present study. Nevertheless, similarities in the way reflected sound effects the air particle velocity can be expected between the natural situation and the situation used in the present study. Assuming no differences between the sound fields on the left and right side of a bee, we measured on one side only. Sound pressure was picked up in the horizontal plane around the bees (N=12) at the same measurement points as the particle velocity (Fig. 1B). The sling-tethered bees showed slight intra-individual variations in the generation of thoracic vibrations during an experiment (average variation: velocity amplitude, ±12.5%; main frequency component, ±3.7%; duration of single pulses, ±12.5%; pulse sequence, ±14.1%). We therefore took the measurements (12 different measurement points above the bees or 24 different measurement points in the horizontal plane around the bees) in an arbitrary sequence to reduce any bias caused by potential differences in signalling due to increasing exhaustion of the bees along with the duration of a recording. Sling-tethered bees generated annoyance buzzing for about 10 min (Hrncir et al., 2008). In the present study, the recordings covered time periods between 3 and 5 min per investigated bee.

To judge the significance of the wings for the transformation of thorax vibrations into particle velocity and sound pressure we clipped the wings close to their base. Immediately after wing ablation, the respective aspect of the sound field was measured again with the sensor at the same positions as before. At all measurement points, the respective sound field was thus measured twice for each individual.

The closest possible distance between the USP-probe and the vibrating bee was 5 mm, which prevented the tethered individuals from getting hold of the sensors and damaging them. The amplitudes of air particle velocity at still closer distances (1, 2, 3 and 4 mm) were extrapolated using a hyperbolic decay function (Regression wizard, SigmaPlot 2001, SPSS Inc., Chicago, IL, USA; see Appendix 1). Extrapolations were only applied to particle velocities because sound pressure is not immediately relevant for any known sensory organ of bees.

Preservation of signal pattern

In order to see the extent to which the temporal pattern of the pulsed thorax vibrations is preserved in airborne signals, we simultaneously recorded the thorax vibrations and the particle velocity generated by sling-tethered bees (N=12 bees). Thorax vibrations were recorded as velocities using a portable Laser Doppler Vibrometer (PDV-100, Polytec, Waldbronn, Germany). The measurement point of the laser vibrometer was on the bee's scutum. The particle velocity was measured at 5 mm and 10 mm behind the vibrating bee, lateral to its thorax and in front of its head. The following parameters were analysed: the duration of single pulses (*PD*), their main frequency component (*MF*), and the pulse sequence (*PS*), which is the time from the onset of one pulse to the onset of the following pulse (Fig. 2).

Jet airflow

To investigate the potential existence of a unidirectional (jet) airflow generated by vibrating bees, we positioned a custom-made hot-wire anemometer sensitive to low frequencies (~1.2mV/[mm s^{-1}]) 5 mm behind a total of six sling-tethered bees (where the jet should occur), and 5 mm laterally of its thorax (where the jet seemed unlikely). Simultaneously, the thorax vibrations of the bees were picked up with a laser vibrometer. The anemometer was placed both behind the bee and laterally to it, for about one minute each. We reduced the influence of ambient air currents within the laboratory by performing the measurements inside a cardboard arena (20×20×10 cm^2). However, sound reflections from the cardboard box, air currents caused by the cooling systems of our equipment (laser vibrometer, notebook), and electrical noise originating from the current supply could not be fully avoided and resulted in background noise equivalent to about 2 mm s^{-1}. Yet, jet airflows if present should still have been detected, as they were reported to reach velocity amplitudes of 150 mm s^{-1} at a distance of 5 mm behind vibrating honey bees (Michelsen, 2003).

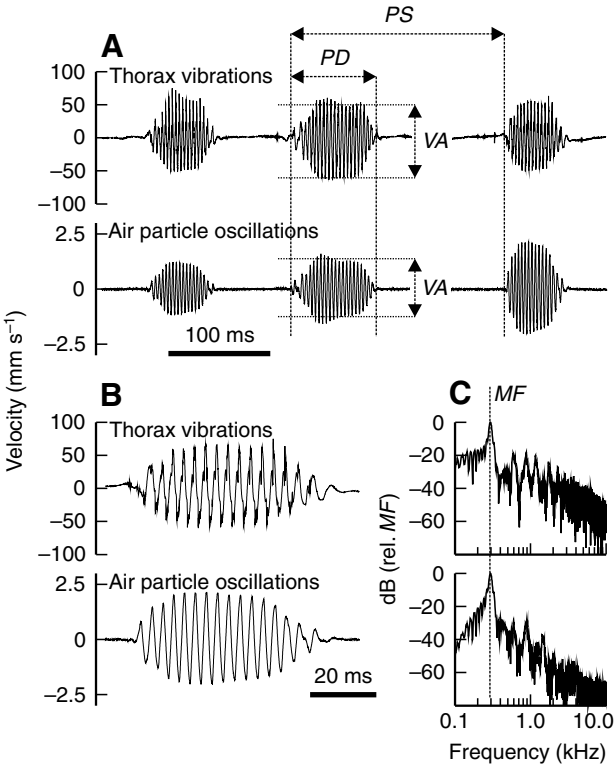

Fig. 2. Simultaneously measured thorax vibrations (laser vibrometer) and air particle velocity (USP-probe). In the case shown here, the USP-probe was 5 mm away from the bee at direction iii (see Fig. 1). (A) Velocity amplitude (*VA*), pulse duration (*PD*), and pulse sequence (*PS*). (B) A single pulse illustrating the close similarity between the thorax vibrations and the air particle oscillations. (C) Frequency power spectra of the pulses shown in B; *MF*, main frequency component.

Distribution of hive bees around vibrating foragers

To see whether hive bees stay within a range around vibrating foragers allowing signal transmission through airborne sound, we videotaped 20 trophallactic interactions of six different foragers (digital video-camera: Panasonic, NV-GS400GE; 30 frames s^{-1}). For these recordings, the foragers (one individual per recording day) had been trained to collect sugar solution (50% cane sugar w/w) at an artificial food source 15 m away from the nest entrance. The video-caption showed the vibrating forager and a ca. 2 cm range around it during trophallaxis. This caption size allowed both a good

view of the distribution of the hive bees around the forager, and exact distance measurements. The recordings were analysed using the software VideoPoint 2.5 (Lenox Softworks Inc., Lenox, MA, USA). Due to their movement and the resulting blurred video-image, it was impossible to identify the exact position of the antennae. Instead, we took the midpoint of the hive bees' heads as a reference to measure their position. We analysed the closest distance to the vibrating forager for those hive bees that were not involved in the food transfer during the respective trophallactic interaction. We only took those hive bees into account that 'showed an interest' in the forager without getting involved into trophallactic food transfer. As a measure for 'being interested' we took the approach towards the forager in a roughly straight line. Several hive bees that just passed by, moved out of the caption, or did not clearly change position during the recording were excluded from the analysis. Because the caption size of the camera had a radius of only about 2 cm, we could not determine at which points the bees decided to move towards the forager. However, our emphasis was to determine whether those hive bees that moved towards the forager do get close enough to the vibrating bee to detect any particle velocity generated by its thoracic vibrations.

Analysis and statistics

The output signals of the USP-probe, the hot-wire anemometer and the laser vibrometer were fed into a notebook (Pentium IV, 2.4 GHz) using a 24-bit stereo soundcard (PSC 805, Philips, Amsterdam, The Netherlands) and the software Soundforge 7.0 (Sony Digital Inc., Madison, WI, USA) at a sampling rate of 44.1 kHz. For the analysis of thorax vibrations and airborne sound we used the softwares SpectraPro 3.32 (Sound Technology Inc., Campbell, CA, USA), SigmaPlot 2001 (SPSS Inc., Chicago, IL, USA) and SigmaStat 3.10 (Systat Software Inc., San Jose, CA, USA).

For each individual, the mean values of sound pressure or air particle velocity at each measurement point were calculated from 15–30 vibratory pulses. The statistical tests were performed with these representative mean values. Because the data were normally distributed in all cases (Kolmogorov–Smirnov test, $P>0.05$) and showed equal variance (Levene median test, $P>0.05$), we applied parametric tests. The Paired *t*-test was used to compare the amplitudes of airborne sounds at each measurement point before and after clipping the wings. One-way repeated-measures ANOVA (*post-hoc* pairwise comparison: Tukey test) indicated possible significant differences between amplitudes measured at the same distance but in different horizontal directions to the vibrating bee. Spearman rank correlation was applied to test the relationship between signal parameters (*PD*, pulse duration; *PS*, pulse sequence; *MF*, main frequency component; *VA*, velocity amplitude) of thorax vibrations and air particle oscillations. The correlation coefficient (r_S) indicates the degree of association between them ($r_S=1$, high association; $r_S=0$, no association). Throughout the text, values are presented as mean ±1 s.d. *N* refers to the number of different individuals tested, and *n* to the number of single pulses evaluated. The level of significance of differences was taken as $P\leqslant 0.05$. A Bonferroni correction for the level of significance was performed ($P_{corr.}\leqslant 0.05$/number of comparisons) (Sokal and Rohlf, 1995) when data sets were used for more than one statistical comparison.

RESULTS

Sound field generated by vibrating bees

Particle velocity

During annoyance buzzing, air particle velocities could be recorded at all measurement points both above and in the horizontal plane around a vibrating bee (Figs 3–6). There were significant differences between the amplitudes picked up at the same distance but in different directions from the vibrating individual (one-way repeated-measures ANOVA: $P_{corr.}\leqslant 0.025$; Tables 1, 2). The highest particle velocity was measured 5 mm above the plane of the wings (16.0±4.76 mm s^{-1}). Here, the velocity amplitude of the air particle oscillations was significantly larger than the highest values measured in the horizontal plane

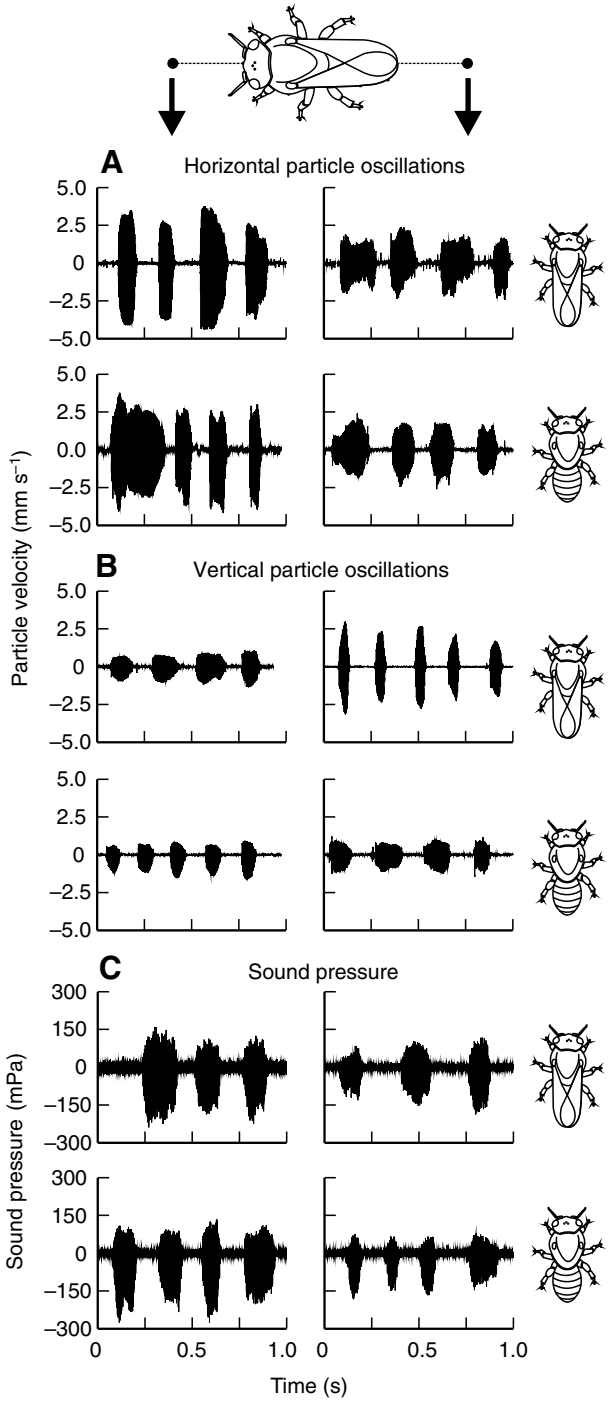

Fig. 3. Typical examples of airborne sound picked up with the USP-probe 5 mm in front of the head (left panels) and 5 mm behind the wingtips/abdomen (right panels). (A) horizontally and (B) vertically oriented air particle oscillations, and (C) sound pressure induced by the thorax vibrations before (upper rows) and after wing ablation (lower rows).

around the bee (vertically oriented oscillations, 5 mm behind the wingtips: 6.0±2.08 mm s^{-1}; horizontally oriented oscillations, 5 mm in front of the head: 8.6±2.95 mm s^{-1}; one-way ANOVA, $F_{2,32}$=26.60, P<0.001) (compare Table 1 with Table 2). Above the bee, the vertically oriented particle velocity steadily decreased between the measurement points above the wings and the measurement points above the head (Fig. 4, Table 1). In the plane around the bee, vertically oriented particle velocity was strongest behind the bee's wingtips and weakest in front of its head at distances ⩽5 mm (values extrapolated from the exponential decay functions given in Appendix 2) (Fig. 5, Table 2). At distances beyond 5 mm, the field of vertical particle velocities was largely homogeneous around the vibrating bee (one-way repeated measures ANOVA: no significant differences between directions; Fig. 5, Table 2). Horizontally oriented particle velocity around the bee was largest in front of the bee's head, and lowest lateral to the bee's thorax at distances ⩾5 mm (Fig. 6, Table 2). Closer to the vibrating bee, at distances <5 mm (values extrapolated from the exponential decay functions given in Appendix 2), the field of horizontally oriented particle oscillations was highly polarised, showing highest velocity amplitudes in front of the bee's head and lowest values behind its wings (direction v; Fig. 6, Table 2). Thus, the polarization of the field of horizontally oriented particle velocity decreased with increasing distance to the vibrating bee, becoming insignificant (P>0.05) at a distance of 20 mm.

Table 1. Mean values of vertically oriented air particle velocity above the head, the thorax and the wings close to the wingtips

Distance (mm)	Particle velocity (mm s^{-1})			$F_{2,30}$	P
	Head	Thorax	Wingtips		
1*	23.54	43.15	**61.46**	–	–
2*	12.55	22.39	**31.62**	–	–
3*	8.56	15.11	**21.29**	–	–
4*	6.49	11.41	**16.05**	–	–
5	5.66^{a}	10.91^{b}	**16.03**^{c}	24.45	<0.001
10	2.05^{a}	3.04^{b}	**3.58**^{b}	14.29	<0.001
15	1.47^{a}	$1.62^{a,b}$	**1.72**^{b}	5.20	0.015
20	1.27	**1.43**	1.37	2.24	0.13 n.s.

Bold letters emphasize highest values at the given distance.
Air particle velocities measured at same distances (⩾5 mm) but at different positions were compared using one-way repeated measures ANOVA (F-values given). Level for significance of difference is $P_{corr.}$⩽0.025. Values in a row that have same superscript letters did not differ significantly from each other (pairwise comparison: Tukey-test, P>0.05); n.s., not significant.
*Values extrapolated from hyperbolic decay function (see Appendix 2).

Sound pressure

Similar to horizontally oriented particle velocity, sound pressure in the plane around the bee was generally highest in front of the bee's head and lowest behind its wingtips (directions v and vi) (Fig. 7, Table 3). The highest sound pressure recorded was at 5 mm in front of the bee's head (323.0±85.6 mPa). Differences between the fields of sound pressure and horizontally oriented particle velocity (compare Table 2 with Table 3; e.g. at a distance of 15 mm to the vibrating bee, the highest sound pressure was recorded laterally of the bee's thorax, and the highest horizontal particle velocity in front of its head) might originate from slight differences in the distance between the vibrating bee and the sensor between different recordings (±1 mm accuracy: see Materials and methods). Alternatively, or in addition, they point to the fact that close to a vibrating bee sound pressure and particle velocity might not be related to each other in a simple way.

The significance of the wings for the generation of the sound field

By removing the bee's wings, we determined their significance for the transformation of thorax vibrations into airborne sounds. According to a comparison of air particle velocity and sound pressure before and after wing removal neither the amplitude of the horizontally

Table 2. Mean values of both vertically and horizontally oriented air particle velocities (p-p) around a vibrating bee, at different distances and directions (i–vi) relative to the vibrating bee

	Distance (mm)	Particle velocity (mm s^{-1}) in directions i–vi						$F_{5,55}$	P
		(i)	(ii)	(iii)	(iv)	(v)	(vi)		
Vertically oriented	1*	7.78	11.98	21.41	17.52	18.48	**25.47**	–	–
	2*	5.65	7.53	11.06	10.09	10.18	**13.25**	–	–
	3*	4.57	5.49	7.46	7.09	7.02	**8.95**	–	–
	4*	3.84	4.32	5.63	5.46	5.36	**6.76**	–	–
	5	3.31^{a}	$3.58^{a,b}$	$4.72^{b,c}$	$4.86^{c,d}$	$4.67^{b,c}$	**6.03**^{d}	11.70	<0.001
	10	2.00	1.82	2.00	2.02	1.93	**2.02**	0.74	0.60 n.s.
	15	1.33	1.26	**1.41**	1.26	1.29	1.33	1.62	0.17 n.s.
	20	1.11	1.11	1.04	**1.16**	1.07	1.13	1.43	0.23 n.s.
Horizontally oriented	1*	**20.84**	10.86	9.92	10.68	9.66	10.88	–	–
	2*	**16.22**	9.15	8.27	8.90	8.21	9.17	–	–
	3*	**12.87**	7.78	6.96	7.50	7.03	7.79	–	–
	4*	**10.39**	6.67	5.92	6.37	6.07	6.68	–	–
	5	**8.57**^{a}	5.82^{b}	5.16^{b}	5.53^{b}	5.34^{b}	5.83^{b}	11.17	<0.001
	10	**3.34**^{a}	$2.82^{a,b}$	2.31^{b}	2.57^{b}	$2.64^{a,b}$	$2.83^{a,b}$	4.17	0.003
	15	**1.98**^{a}	$1.76^{a,b}$	1.48^{c}	$1.54^{b,c}$	$1.70^{b,c}$	$1.76^{a,b}$	7.85	<0.001
	20	**1.55**	1.44	1.35	1.41	1.36	1.43	1.76	0.14 n.s.

See Fig. 1B for details on directions i–vi.
Bold letters emphasize highest values measured at the given distance.
Particle velocities measured at the same distances (⩾5 mm) but in different directions were compared using one-way repeated measures ANOVA (F-values given). Level for significance of difference: $P_{corr.}$⩽0.025. Values in a row that have same superscript letters did not differ significantly from each other (pairwise comparison: Tukey-test, P>0.05); n.s., not significant.
*Values extrapolated from hyperbolic decay function (see Appendix 2).

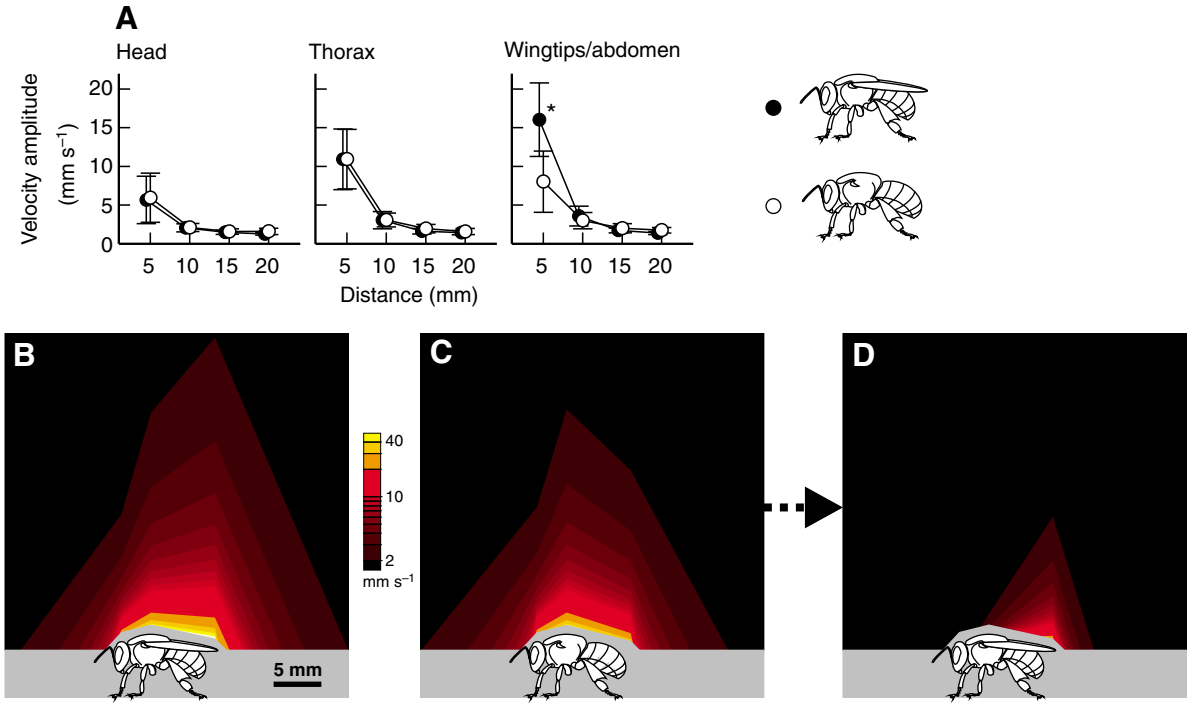

Fig. 4. Vertically oriented air particle velocity amplitude *VA* (p-p) above a vibrating bee. (A) Mean values ±1 s.d. (*N*=11) above head, thorax and wingtips/abdomen, before (filled circles) and after wing removal (open circles). Circles are slightly displaced horizontally for better visibility. Asterisk indicates significant difference (paired *t*-test; $P_{corr.}\leqslant 0.025$) between intact and wingless bees. (B–D) Ranges above the vibrating bee in which air particle velocities had the same mean amplitudes (extrapolated from hyperbolic decay functions, see Appendix 2). Different colours indicate mean velocity amplitudes between 2 mm s^{-1} and 40 mm s^{-1} as explained by the logarithmic colour scale. (B) Intact individuals, (C) wingless individuals, (D) portion of particle velocity generated solely by wings (see text for details). Values for directions in front and behind of the bee were taken from vertically oriented particle oscillations in Fig. 7. Shaded area above bee marks the 1 mm range that cannot be accurately described by decay functions (see Appendix 1). Because the airflow sensors were positioned at least 5 mm above the substrate, no values are given for the region below 5 mm (shaded area).

oriented particle velocity nor the sound pressure were significantly influenced (paired *t*-test: $P_{corr.}>0.025$; Figs 6 and 7). Yet, removing the wings reduced the amplitude of vertically oriented particle velocity above and behind the abdomen. However, this effect was statistically significant only at a distance of 5 mm from the vibrating individuals (paired *t*-test: $P_{corr.}<0.025$; Figs 4 and 5).

To determine which portion of the particle velocity is generated solely by the oscillating wings, we subtracted each bee's mean particle velocity generated after wing removal from its 'intact' value. Again, an exponential decay function was applied to extrapolate particle velocity values close to the bees. As shown in Figs 4 and 5, the significance of the wings for vertical particle oscillations (above and around a bee) was restricted to the immediate neighbourhood of the wings, and the abdomen, respectively. The oscillating wings were responsible for a part of the horizontal particle oscillations measured laterally to the bee and in front of it (Fig. 6). Compared to the effect on vertically oriented particle oscillations, however, this effect was very small.

Preservation of temporal signal patterns

According to previous studies (Hrncir et al., 2006a), the potential signal value of air movement (sound) should depend on the extent to which the temporal pattern of the thorax vibrations is preserved after its transformation into particle velocity. At all measurement points around a vibrating bee (directions i, iii and vi, at both 5 and at 10 mm distance from the individual) the temporal pattern of the air particle oscillations highly correlated with that of the thorax vibrations (5 mm, Spearman rank correlation, i: $r_{S,PD}$=0.96, $r_{S,PS}$=1.00, $r_{S,MF}$=0.98, N=12, n=156; iii: $r_{S,PD}$=0.97, $r_{S,PS}$=1.00, $r_{S,MF}$=0.98, N=12, n=155; vi: $r_{S,PD}$=0.96, $r_{S,PS}$=1.00, $r_{S,MF}$=0.91; N=12, n=183; 10 mm, Spearman rank correlation, i: $r_{S,PD}$=0.96, $r_{S,PS}$=1.00, $r_{S,MF}$=0.94, N=12, n=142; iii: $r_{S,PD}$=0.93, $r_{S,PS}$=1.00, $r_{S,MF}$=0.95, N=12, n=153; vi: $r_{S,PD}$=0.95, $r_{S,PS}$=1.00, $r_{S,MF}$=0.96; N=12, n=152).

Vibrating stingless bees do not generate jet airflows

The possible existence of jet airflows generated by vibrating stingless bees was tested by measuring the air particle movement behind the wingtips (direction vi) and laterally of the thorax (direction iii) at a distance of 5 mm. In honey bees, the wing movements going along with the thorax vibrations during the waggle dance were found responsible for the generation of an air jet with velocity amplitudes of up to 150 mm s^{-1} behind the wingtips (Michelsen, 2003). In *M. scutellaris*, no obvious differences existed between the position behind the vibrating bee and the lateral position (Fig. 8). Despite the strong background noise in our recordings (Fig. 8), a strong, unidirectional jet airflow would have been detected if present. However, the recordings made behind and laterally to the bees did not differ.

Distribution of hive bees around vibrating foragers

During 20 trophallactic interactions, we determined the closest distance between 128 hive bees and the vibrating foragers (*N*=6). In 77.3% of the observed cases (99 individuals), the heads of the hive bees were closer than 5 mm to the forager, and in only 3.1%

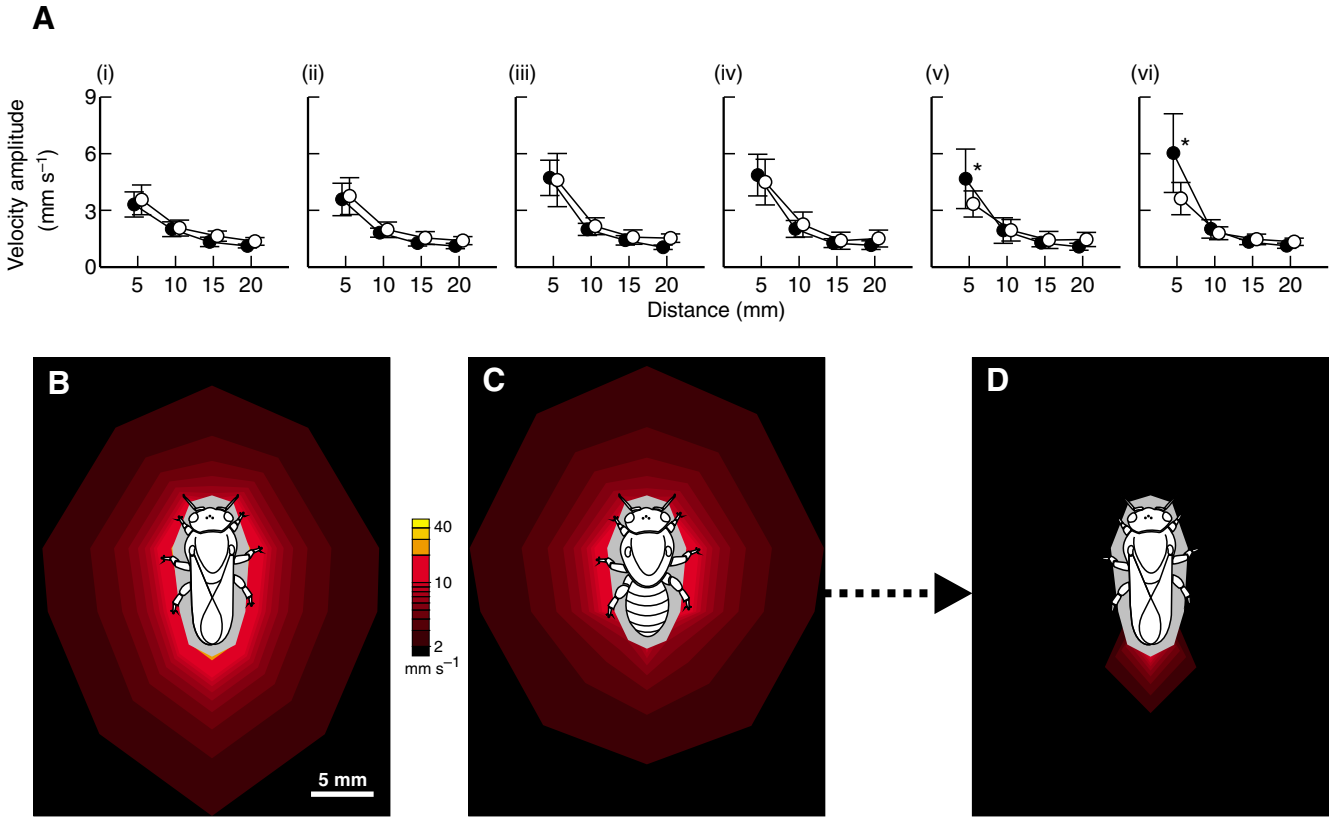

Fig. 5. Vertically oriented air particle velocity amplitude *VA* (p-p) around a vibrating bee. (A) Mean values ±1 s.d. (*N*=12) picked up 5, 10, 15 and 20 mm from the vibrating bees and at measurement points in different directions relative to the long axis of the bee (i–vi; see Fig. 1B); values before (filled circles) and after wing removal (open circles). Circles are slightly displaced horizontally for better visibility. Asterisks indicate significant difference (paired *t*-test; $P_{corr.} \leqslant 0.025$) between intact and wingless bees. (B–D) Ranges around the vibrating bee with particle velocities of the same mean amplitudes (extrapolated from hyperbolic decay functions, see Appendix 2). Colour scale as in Fig. 4. (B) Intact individuals, (C) wingless individuals, (D) particle velocity generated only by wings (see text for details). Shaded area around bee: marks the 1 mm range that cannot be accurately described by decay functions (see Appendix 1).

of the cases (4 individuals), the bees stopped moving towards the forager at distances larger than 10 mm (Fig. 9). The majority of the hive bees (76.6%, 98 individuals) took a position lateral to the foragers. The antennal tips of all bees less than 5 mm away from the forager were certainly able to touch the forager's body (Fig. 9A). According to observations without video-equipment (D.L.P., unpublished), hive bees indeed do touch a vibrating forager's body with their antennae.

DISCUSSION

Generation of airborne sound

In bees there seem to be at least two different ways to transform thorax vibrations into airborne sounds. Whereas in honey bees the wings are important for this transformation, in stingless bees and bumble bees (Schneider, 1975) the structure responsible for the generation of airborne sounds is predominantly the vibrating thorax itself.

A simple comparison of the distribution of sound pressures produced by a vibrating stingless bee (*M. scutellaris*) and a honey bee (*Apis mellifera*), already suggests a difference in the respective generation of the sound fields. In the dancing honey bee, sound pressure was as high as *P*=156 mPa 10 mm behind its abdomen, and as high as *P*=127 mPa lateral to its wings (Esch, 1961). No sounds could be heard in recordings made in front of the head, which was taken to indicate that airborne sounds are generated by the oscillating wings (Esch, 1961; Wenner, 1962). This is supported by findings of Michelsen et al. (Michelsen et al., 1987). After removing the wings from one body side, the sound pressure measured laterally on the winged side was 3–4 times higher than that on the wingless side. With all four wings removed, the amplitude of the sound decreased to values below the sensitivity of the pressure microphone located 2 mm above the bee's abdomen (Michelsen et al., 1987).

In *M. scutellaris*, the sound pressure behind the wingtips of vibrating sling-tethered individuals was very similar to that measured in honey bees (direction vi, 10 mm distance to wingtips: *P*=151 mPa, Table 3). However, different from honey bees, sound pressure could be measured all around an individual and even reached its maximum in front of its heads (Fig. 7, Table 3). Clipping the wings did not affect sound pressure (Fig. 7). Apparently, in *M. scutellaris* the wings do not play a significant role in the transformation of thoracic vibrations into sound pressure. Similarly, in bumble bee queens emitting a pulsed defence buzzing when tethered (Schneider, 1975), sound pressure could be recorded behind, laterally and in front of the vibrating individuals. Unfortunately, sound pressure values for the different positions around the bee are not provided in this publication (Schneider, 1975). However, similar to our findings, the sound pressure did not change in general in amplitude following the removal of the wings (Schneider, 1975).

Air particle movement

The physical parameter most relevant for the sensory perception of airborne sound by bees is air particle movement. In dancing honey

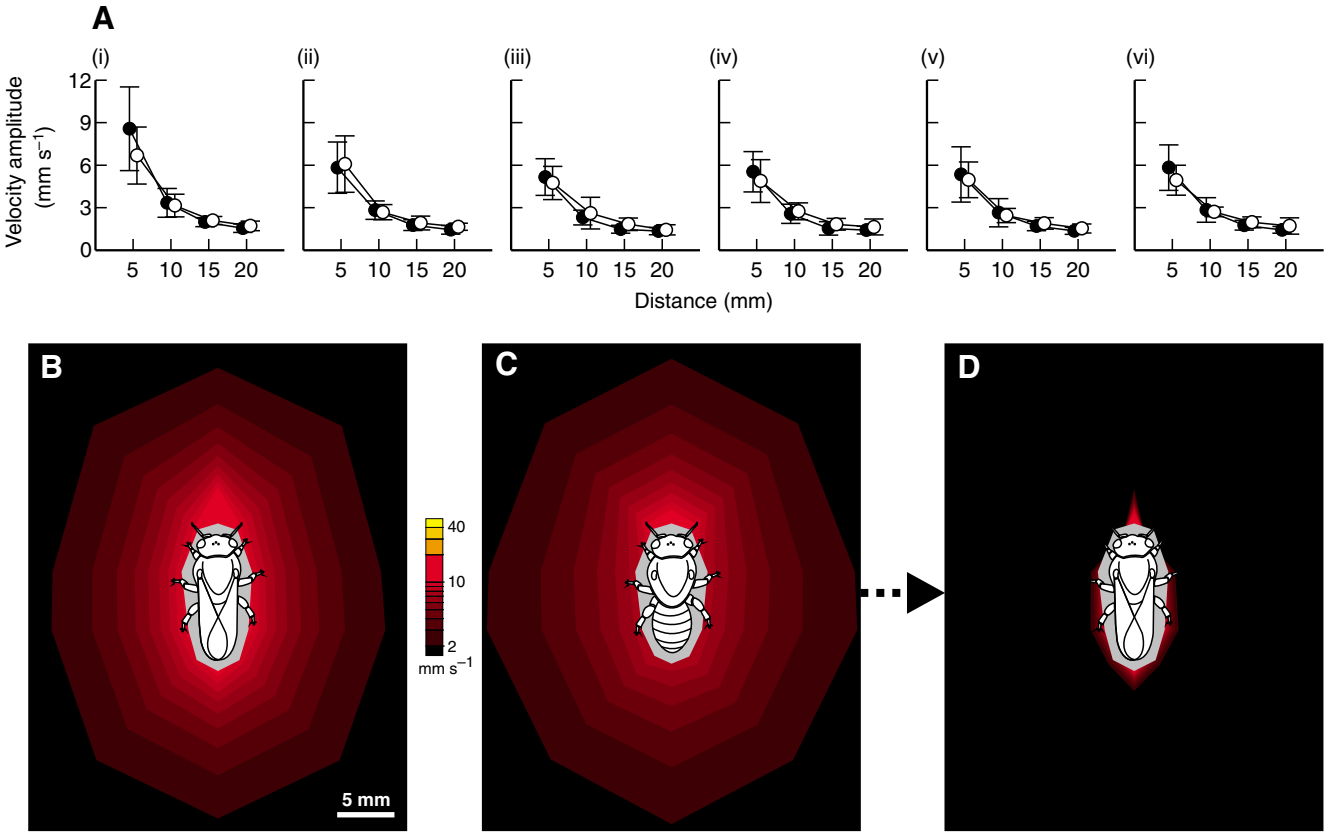

Fig. 6. Horizontally oriented particle velocity amplitude *VA* (p-p) around a vibrating bee. (A) Mean values ±1 s.d. (*N*=12) at distances of 5, 10, 15 and 20 mm from the vibrating bees at measurement points in different directions relative to the long axis of the bee (i–vi; see Fig. 1B); values before (filled circles) and after wing removal (open circles). Circles are slightly displaced horizontally for better visibility. There were no significant changes of values after wing ablation (paired *t*-test; $P>P_{corr}$, 0.025). (B–D) Ranges around the vibrating bee where particle velocities had the same mean amplitudes (extrapolated from hyperbolic decay functions, see Appendix 2). Colour scale as in Fig. 4. (B) Intact individuals, (C) wingless individuals, (D) portion of particle velocity generated solely by wings (see text for details). Shaded area around bee marks the 1 mm range that cannot be accurately described by decay functions (see Appendix 1).

bees, two different forms of air particle movement have been described. First, the oscillating wings create intense air particle oscillations close to their edges (Michelsen et al., 1987). Second, air that moves out from the space between the wings and the abdomen during wing vibrations creates an air jet moving away from the bee's abdomen (Michelsen, 2003). Both these forms of air particle movement in the honey bee depend on the wing oscillations that go along with the thoracic vibrations. In *M. scutellaris*, particle velocity, similar to sound pressure, was predominantly generated by the thoracic oscillations. As expected, oscillations of the wings significantly affected the vertically oriented particle velocity close to the abdomen only (Figs 4–6).

The differing importance of the wings for the generation of the sound field in *A. mellifera* and *M. scutellaris*, respectively, is thought to be due to a difference in wing position. Whereas honey bees generate sounds with splayed wings during their dance movements, with the wing tips 5–9 mm apart (Michelsen, 2003), stingless bees generate thorax vibrations during both forager vibrations and annoyance buzzing with their wings closely folded over the abdomen (Lindauer and Kerr, 1958; Hrncir et al., 2006a; Hrncir et al., 2006b; Hrncir et al., 2008). Due to the folding of the wings, these are uncoupled from the indirect flight mechanism and, thus, their oscillation amplitude during 'buzzing' is strongly reduced compared to that during flight (Heinrich, 1993; King et al., 1996). A spreading of the wings increases the effective wing area (Schneider, 1975) which, in turn, increases the amount of air between the wings and the abdomen which is moved by every wing stroke. Wing position probably also influences the way how the air is expelled from this space as indicated by the observation that the splaying of the wings is essential for the generation of the honey bee's jet airflow. A unidirectional airflow behind a dancing honey bee could only be measured when the dancer's wingtips had a distance of at least 2.5 mm from each other (Michelsen, 2003). In accordance with this, no jet airflow could be measured behind vibrating *M. scutellaris* (Fig. 8), which generates sound with its wings completely folded over the abdomen.

Use of airborne sounds for information transfer

In *Melipona* bees, the temporal pattern of the forager's thoracic vibrations predominantly depends on the sugar concentration of the collected food (Hrncir et al., 2006a). The airborne sound going along with the thoracic vibrations was repeatedly assumed to transmit information to the nestmates although particle velocity had not been measured in these studies (Esch, 1967; Nieh et al., 2003). Whereas the temporal pattern of the thorax vibrations (pulse duration, pulse sequence and main frequency component) is indeed well preserved in the airborne sounds [sound pressure (Hrncir et al., 2004a); air particle oscillations, present study] the crucial question whether the air particle velocity close to a vibrating bee is strong enough to be detected by the hive bees is still not answered yet.

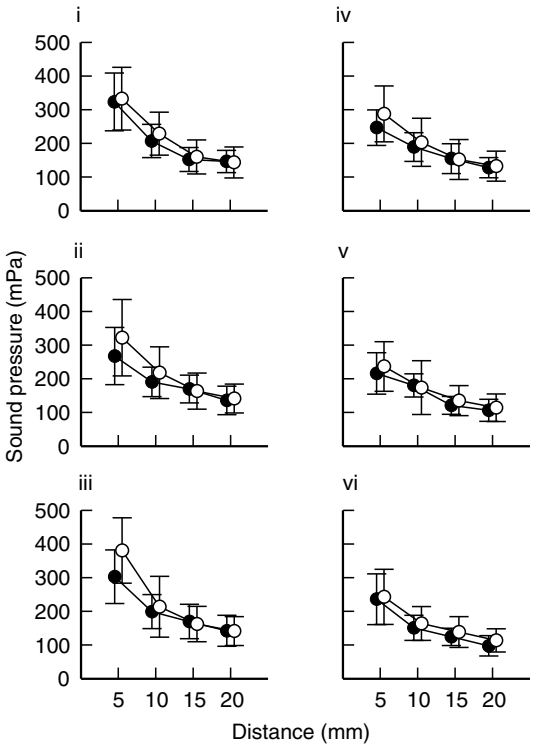

Fig. 7. Sound pressure (p-p) around a vibrating bee. (A) Mean values ±1 s.d. (N=12) measured at distances of 5, 10, 15 and 20 mm from the vibrating bees and at measurement points in different directions relative to the long axis of the bee (i–vi; see Fig. 1B); values before (filled circles) and after wing removal (open circles). Circles are slightly displaced horizontally for better visibility. Sound pressures generated by a bee before and after wing removal do not differ significantly between intact and wingless bees (paired t-test; $P>P_{corr}$, 0.025).

The candidate mechanosensory organ able to detect particle velocity is Johnston's organ in the antennal pedicel, which is stimulated by the deflection of the flagellum (Snodgrass, 1956; Heran, 1959; Tsujiuchi et al., 2007). To date, neither the physiological nor the mechanical properties of this mechanoreceptor are known in stingless bees. A comparison with data available for the honey bee may be helpful, nevertheless. It has only recently been demonstrated (Tsujiuchi et al., 2007) that the minimum displacement amplitude of the honey bee's flagellar tip necessary to elicit a neural response of Johnston's organ is 20 nm, achieved by a free-field air particle displacement of 60 nm. The magnitude of the sound-evoked compound potentials of Johnston's organ linearly increased with antennal tip displacements up to 100 nm. At a flagellar tip displacement above 200 nm, corresponding to a free-field air particle displacement amplitude larger than 5 μm, the magnitude of the neural response reached a saturation level (Tsujiuchi et al., 2007).

Adopting these findings for the recruitment communication of *M. scutellaris*, we conclude that stingless bees in the nest should be able to detect the particle velocities generated by foragers with their antennal mechanoreceptors. Taking the honey bee values, the minimum free-field particle velocities that can be detected by the bees are between 0.13 mm s^{-1} at a frequency of 350 Hz and 0.21 mm s^{-1} at 550 Hz [frequency range of *M. scutellaris* forager vibrations (Hrncir et al., 2000)], corresponding to a particle displacement of 60 nm (free-field) at these frequencies. Saturation of Johnston's organ is reached at free-field particle velocities between 11.0 mm s^{-1} (350 Hz) and 17.2 mm s^{-1} (550 Hz), corresponding to a particle displacement of 5 μm at these frequencies.

Due to the difficulties in accurately positioning sensors around vibrating foragers during their trophallactic interactions with hive bees, it is an almost impossible task to properly measure particle velocities induced by forager vibrations close to the receiver bee. Forager vibrations, however, are very similar in terms of the mechanism of their generation to annoyance buzzing. Both types of thoracic vibrations result to a similar degree in oscillations of the legs and of the wingtips (Hrncir et al., 2008). Therefore, the study of annoyance buzzing can give an insight into signals generated during forager vibrations. Yet, the velocity amplitudes of thoracic vibrations by foragers are about 55% of those during annoyance buzzing (Hrncir et al., 2008). Since the particle velocity depends on the velocity amplitude of the sound source (Appendix 1), we must take into account that the particle velocities generated by vibrating foragers might be only about half of the values recorded in the present study. Even so, and despite the complexities of the physics of sound generation close to a structure like a vibrating thorax, hive bees of *M. scutellaris* should be able to detect forager generated particle velocities within a range of at least 2 cm from the vibrating bee (smallest measured particle velocity at 2 cm from a sling-tethered bee: 1.04 mm s^{-1} → 0.52 mm s^{-1} induced through forager vibrations). At distances smaller than 5 mm from the vibrating bee, the particle velocity generated by foragers will even result in the maximum response of Johnston's organ neurons. The maximum particle velocities found in the present study were 25.5 mm s^{-1} (first standard deviation: ±8.7 mm s^{-1}) at 1 mm behind the vibrating bee (→12.8 mm s^{-1} in behind the forager), 43.2 mm s^{-1} (±15.6 mm s^{-1}) at 1 mm above the thorax (→21.6 mm s^{-1} above the forager's thorax), and 61.5 mm/s (±18.5 mm s^{-1}) at 1 mm above the wings (→30.8 mm s^{-1} above the forager's wings). Hive bees that attended trophallactic events stayed predominantly within <5 mm from the vibrating forager (Fig. 9) and their splayed antennae were close to or indeed touching the forager (Fig. 9A). Similarly, in *M. panamica* the antennal tips of hive bees were within a distance of at most 2 mm from the vibrating forager's body during trophallaxis, and in about 30% of the cases the antennal tips were above the wings or

Table 3. Mean values of sound pressure (p-p) measured at the given distances and directions (i–vi) relative to the vibrating bee

Distance (mm)	Sound pressure (mPa) in directions i–vi						$F_{5,55}$	P
	(i)	(ii)	(iii)	(iv)	(v)	(vi)		
5	**323.0**^{a}	267.4^{a,b}	302.7^{a,b}	246.7^{b,c}	215.8^{c}	236.0^{b,c}	6.25	<0.001
10	**207.1**^{a}	190.6^{a,b}	199.1^{a}	189.1^{a,b}	180.2^{a,b}	151.0^{b}	3.49	0.008
15	152.0^{a,b}	169.6^{a}	**169.9**^{a}	154.8^{a,b}	120.9^{b}	124.2^{b}	6.51	<0.001
20	**146.2**^{a}	135.6^{a}	142.2^{a}	127.7^{a,b}	106.4^{b,c}	97.5^{c}	8.94	<0.001

See Fig. 1B for details on directions i–iv.

Bold letters emphasize highest measured values at the given distance.

Sound pressures measured at same distances (⩾5 mm) but in different directions were compared using one-way repeated measures ANOVA (F-values given). Level for significance of difference is $P_{corr.}\leqslant 0.025$. Values in a row that have same superscript letters did not differ significantly from each other (pairwise comparison: Tukey-test, $P>0.05$).

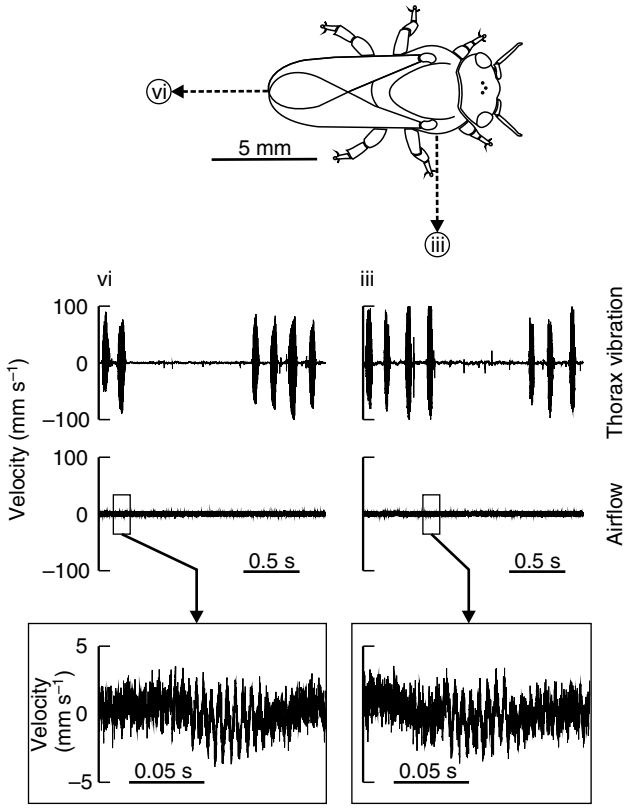

Fig. 8. Simultaneously measured thorax vibrations and unidirectional air movements. A jet airflow was only to be expected behind the vibrating bees (see text). The airflow recordings made 5 mm behind the wingtips (direction vi relative to the long axis of the bee, see Fig. 1), and those made 5 mm laterally (direction iii relative to the long axis of the bee; see Fig. 1) did not differ. Scaling for the airflow was chosen in accordance with the velocity amplitude of the air jet described in honey bees, 150 mm s^{-1} (Michelsen, 2003). Insets: amplified vibratory pulses showing air particle oscillations along with the thorax vibrations.

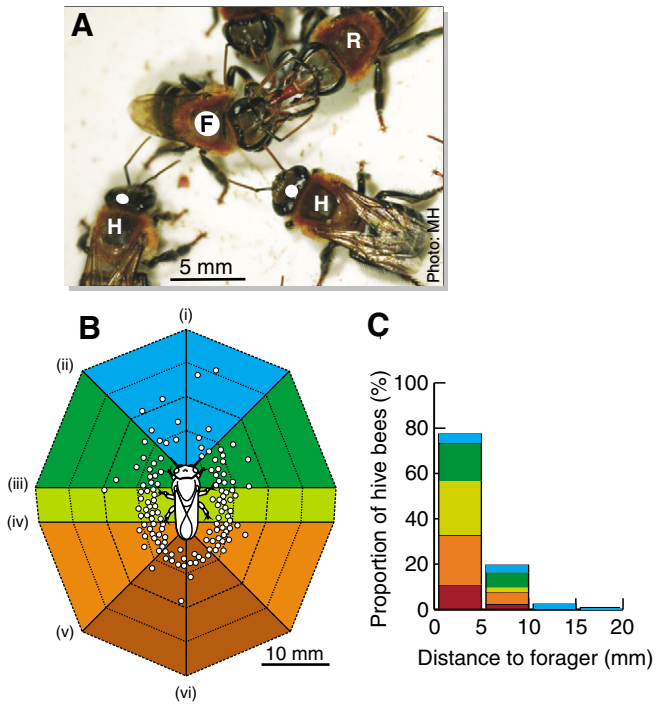

Fig. 9. Distribution of hive bees (H) around a vibrating forager (F) during trophallactic food transfer measured within a circle of 2 cm radius around the centre of the forager's thorax. Food receivers (R) were not included in the analysis. The closest position between the heads of hive bees (midpoint indicated by white dot) and the foragers served as a measure for the distance. (B,C) Distribution of 128 hive bees attending 20 trophallactic interactions (six different foragers). Different colours represent different regions around vibrating foragers; the borderlines between different regions correspond to directions (i–vi) given in Fig. 1B.

the thorax of the forager (Nieh, 1998). In the case of physical contact between the hive bees' antennae and the body of a forager, the thoracic vibrations will be directly transmitted. The thoracic vibrations will then be a stronger stimulus for Johnston's organ than the air particle velocity around the bees (see Appendix 1).

In addition to using the temporal pattern of the airborne sounds (which highly correlates with the temporal pattern of the forager's thoracic vibrations) as information on the profitability of the food source (Hrncir et al., 2004a), hive bees could use any air particle movements to detect an active forager in the darkness of the hive. This information is important for both nectar processing bees and inactive foragers (Biesmeijer et al., 1998; Anderson and Ratnieks, 1999). Thus, airborne sound may transmit different kinds of information. Electrophysiological studies of the responses of the appropriate mechanoreceptors in stingless bees are needed to answer this question.

APPENDIX 1

Particle velocity radiated from spherical sound sources

Due to its complex oscillation movements, which are a result of the interplay between different parts of the cuticle and the thoracic muscles, not to mention the effects of oscillating wings and the head, the bee's thorax is far from representing a simple sound source. Nevertheless, calculations of sound radiated by theoretical sound sources (Morse, 1981; Jacobsen et al., 2007) might help to get more quantitative understanding of the air particle velocities very close to the bees, where measurements were not possible. The models that come closest to a vibrating thorax are a monopole (pulsating sphere), and a dipole (sphere vibrating along polar axis).

Radiation of sound from monopole sources

The simplest sort of outgoing sound wave is from a uniformly expanding and contracting sphere of radius a. The particle velocity u at distance r from the center of the sphere (r=a+d) at the frequency v is (Jacobsen et al., 2007):

$$|u_{r(v)}| = \frac{Q_{(v)}}{4\pi}\,\frac{\sqrt{k_{(v)}^2 r^2+1}}{r^2}\,, \qquad \text{(A1)}$$

($Q_{(v)}$, source strength; $k_{(v)}$=$2\pi v/c$; r, distance from the center of the sphere; u, air particle velocity; v, oscillation frequency).

Knowing the velocity amplitude at the surface of the sphere (r=a) for a given frequency ($U_{0(v)}$), we can determine $Q_{(v)}$:

$$Q_{(v)} = \frac{4\pi a^2 U_{0(v)}}{\sqrt{k_{(v)}^2 a^2+1}}\,, \qquad \text{(A2)}$$

(a, radius of the sphere; U_0, velocity amplitude at the surface of the sphere).

From the combination of the Eqn A1 and A2 results:

$$|u_{r(v)}| = \frac{U_{0(v)}a^2}{\sqrt{k_{(v)}^2a^2+1}} \frac{\sqrt{k_{(v)}^2r^2+1}}{r^2} . \quad (A3)$$

For the radiation of sound from the bee's thorax considered a sphere with monopole character, Eqn A3 can be transformed to:

$$VA_d = \frac{VA_{Tx}a^2}{(a+d)^2} \sqrt{\frac{k_{(MF)}^2(a+d)^2+1}{k_{(MF)}^2a^2+1}} , \quad (A4)$$

(a, radius of the thorax; d, distance from the thorax; VA_d, peak to peak air particle velocity at distance, d; VA_{Tx}, velocity amplitude p-p of thoracic vibrations; $k_{(MF)}=2\pi MF/c$; MF, main frequency component).

Because:

$$\sqrt{\frac{k_{(MF)}^2(a+d)^2+1}{k_{(MF)}^2a^2+1}} \approx \frac{(a+d)}{a} , \quad (A5)$$

Eqn A4 can be simplified as:

$$VA_d = \frac{VA_{Tx}a}{(a+d)} . \quad (A6)$$

Radiation from dipole sources

If the center of a sphere oscillated along the polar axis with a velocity of $U_0e^{-2\pi ivt}$, the radial velocity of the surface of the sphere is $U_0\cos\upsilon e^{-2\pi ivt}$, where υ is the angle from the polar axis. Close to the source, if $r\rightarrow 0$, the particle velocity u at the distance r from the center of the sphere ($r=a+d$) at the frequency v is (Morse, 1981):

$$|u_{r(v)}| = \left(\frac{2K_{(v)}}{\rho c}\right)\left(\frac{1}{k_{(v)}r}\right)^3 \cos\upsilon e^{-2\pi ivt} , \quad (A7)$$

(c, wave velocity; e, Euler's number; K, constant; t, time; υ, angle from the polar axis; ρ, density of air).

If the radius (a) of the sphere is small compared to the wavelength (which is the case with the thorax of bees), the constant $K_{(v)}$ can be approximated as (Morse, 1981):

$$K_{(v)} \approx \left(\frac{4\pi^3\rho v^3a^3U_{0(v)}}{c^2}\right) . \quad (A8)$$

The radial velocity $u_{(v)}$ at $r=a$ (the surface of the sphere) is (Morse, 1981):

$$|u_{(v)}| = U_{0(v)}\cos\upsilon e^{-2\pi ivt} . \quad (A9)$$

Considering the thorax as sphere, and the radial velocity $u_{(v)}$ at its surface as VA_{Tx}, the peak to peak particle velocity VA_d at distance d from the surface of the sphere can be estimated through a combination of Eqn A7–A9:

$$VA_d = \frac{VA_{Tx}a^3}{(a+d)^3} . \quad (A10)$$

Comparison between calculated and measured particle velocity

For calculations of the particle velocity radiated from monopole (Eqn A6) and dipole sources (Eqn A10), the radius of the sound source, its vibration velocity, and the main frequency component of the vibrations are required. From the laser-vibrometer recordings in *M. scutellaris*, we can determine these two vibration parameters only for the dorsal surface of the thoracic scutum. We assumed the thorax of the bee to be a sphere with the radius a=1.7 mm (mean ± 1 s.d. from 17 bees=1.70±0.07 mm; vertical thoracic diameter divided by two). The velocity amplitude p-p of the thoracic oscillations was VA_{Tx}=188 mm s^{-1} (mean ± 1 s.d.=187.8± 95.2 mm s^{-1}; N=15, n=120). When comparing the measured particle velocity values to the theoretical values, the difficulties to describe the vibrating bee as a simple sound source become obvious (Fig. A1). Considering the bee's thorax as simple monopole source overestimates the measured values, and considering it as simple dipole source underestimates them.

Regressions calculated from measured values

The closest possible distance between the USP-probe and the vibrating bee was 5 mm, which prevented the tethered individuals from getting of the sensors and damage them. Therefore, the amplitudes of air particle velocity at still closer distances (1, 2, 3 and 4 mm) had to be extrapolated using a regression analysis (Regression wizard, SigmaPlot 2001, SPSS Inc., USA). We applied two hyperbolic decay functions (Fig. A1) that were mathematically closest to the equations for simple monopole sources (compare Eqn A6 and Eqn A11) or simple dipole sources (compare Eqn A10 and Eqn A12).

$$VA_d = \frac{xy}{y+d} , \quad (A11)$$

$$VA_d = \frac{xy^3}{(y+d)^3} , \quad (A12)$$

where VA_d is the air particle velocity (p-p) at distance d and x and y are function variables, calculated by the regression analysis through iteration.

The function variables (x, y), calculated by the regression analysis, should therefore represent the velocity amplitude of the thorax (VA_{Tx}) and the radius a of the sound source. For the

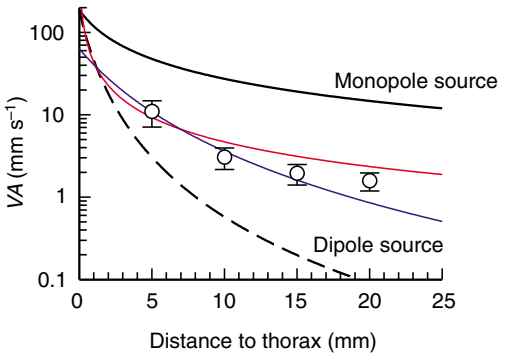

Fig. A1. Theoretical and measured radiation of sound from the thorax of a bee. Line graphs represent particle velocity (VA) as a function of the distance from the thorax, which was assumed to be a monopole source (continuous line) or a dipole source (broken line). Open circles, means (± 1 s.d.) of the particle velocities determined experimentally above the thorax in the present study. Hyperbolic decay functions (hyperbolic decay 1, red line; hyperbolic decay 2, blue line) were calculated from the measured values through regression analysis.

hyperbolic decay function 1 (Eqn A11), the variables were: x=556 (=VA_{Tx}) and y=0.09 (=a). For the hyperbolic decay function 2 (Eqn A12) the variables were: x=63 (=VA_{Tx}) and y=6.26 (=a).

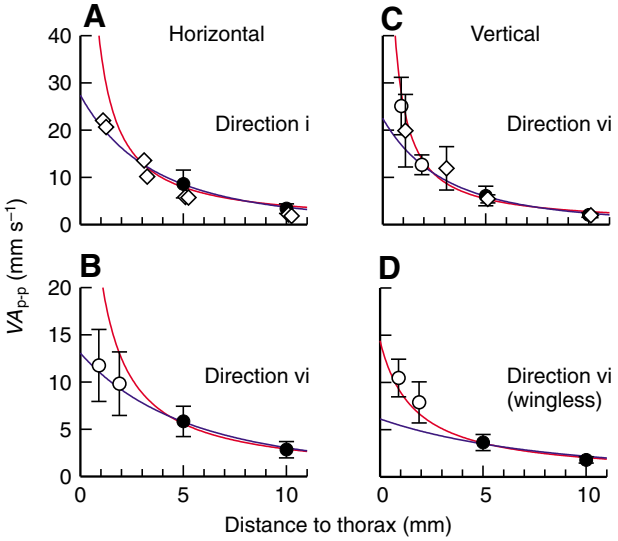

Fig. A2. Extrapolation of air particle velocities close to a bee from exponential decay functions. Horizontally oriented particle velocity in front of a bee (A) and behind a bee (B); vertically oriented particle velocity behind an intact individual (C) and behind a vibrating bee without wings (D). Measurements were made at 1, 3, 5 and 10 mm distance to vibrating individuals of *M. seminigra* (open diamonds; A, N=2, single values shown; C, N=5), and at 1 and 2 mm distance to vibrating *M. scutellaris* (open circles; B, N=5; C, N=5; D, N=4). The values (means ± 1 s.d.) are superimposed onto respective measurements in *M. scutellaris* (filled circles; N=12) and the resulting exponential decay functions (hyperbolic decay 1, red lines; hyperbolic decay 2, blue lines). Some symbols are slightly displaced horizontally for better visibility.

As can be seen from these values, decay function 1 demands a thoracic vibration velocity almost three times stronger than the actual value measured (and a source radius about 20 times smaller), and decay function 2 one that is three times weaker (sound source 4× bigger). Therefore, even if both applied regression functions fit well to the measured particle velocity at distances >5 mm from the vibrating bee (regression coefficients: R^2=70% and 78%), they not necessarily result in reasonable values at distances closer than 5 mm.

To assess the quality of the fit between our data and the regression functions at distances between 1 mm and 5 mm from the vibrating bee, we used data of preliminary experiments made in March 2005 with *M. scutellaris* and *M. seminigra*. The particle–velocity-sensor distances to the vibrating bee had then incautiously been chosen to be 1, 2, 3, 5 and 10 mm, which led to the damage of the sensor by the bees. However, the few results nevertheless received were now compared to the mathematical functions derived from the present study (Fig. A2). Both applied regressions fit well to either the horizontally or the vertically oriented particle velocities (Fig. 2A). Whereas the hyperbolic decay 1 (Eqn A11) describes well the vertically oriented particle velocities, the hyperbolic decay 2 (Eqn A12) is more appropriate for the description of the horizontally oriented particle velocities at close distances (⩾1 mm). In the present study we, therefore, used the hyperbolic decay 1 (which is mathematically similar to the decay around a monopole source) to calculate vertical particle velocities at distances between 1 and 4 mm from the vibrating bee, and hyperbolic decay 2 (mathematically similar to the decay around a dipole source) to calculate the horizontal particle velocities at these distances. However, since it is impossible to describe air particle velocities very close to a vibrating thorax with simple mathematical functions, particle velocities for distances <1 mm from the vibrating bee were not calculated.

APPENDIX 2

Parameters for hyperbolic decay functions calculated for the particle velocity above and around a bee at the respective direction relative to the intact or wingless bee

		Intact			Wingless		
	Direction	x	y	R^2 (%)	x	y	R^2 (%)
Above bee							
Vertically oriented*	He	189	0.14	55	175	0.16	53
	Tx	597	0.08	68	556	0.09	69
	Wt/Abd	1084	0.06	69	336	1.36	58
Around bee							
Vertically oriented*	(i)	11	2.26	82	9	3.31	76
	(ii)	29	0.69	82	13	2.03	73
	(iii)	333	0.07	88	54	0.46	72
	(iv)	66	0.36	83	56	0.43	72
	(v)	101	0.23	72	8	3.69	66
	(vi)	327	0.08	72	14	1.65	76
Horizontally oriented**	(i)	27	10.48	76	15	16.28	76
	(ii)	13	15.98	75	13	15.94	72
	(iii)	12	14.98	81	9	22.08	69
	(iv)	13	14.99	79	9	23.18	68
	(v)	11	16.93	67	9	20.69	75
	(vi)	13	15.97	78	8	24.20	77

He, above head; Tx, above thorax; Wt/Abd, above wingtips or abdomen; around the bee (i-vi), see Fig. 1B.
Decay functions: *$VA_d=xy/y+d$; **$VA_d=xy^3/(y+d)^3$ (see Appendix 1). VA_d, particle velocity, p-p, at distance d; x, y: function variables.

We would like to thank Luci Rolandi Bego and Ana Carolina Roselino for kindly making the colonies of *M. scutellaris* available. We also thank Christian Klopsch and Karina Jorke for comparing the USP-probe measurements with the PIV measurements, and Hans-Elias de Bree (Microflown Technologies) for information and discussions about the Microflown™ USP-sensor. The experiments comply with the current laws of Brazil, where they were performed. This study was supported by FWF grant P17530 to F.G.B. M.H. is currently supported by FAPESP grants 06/50809-7 and 06/53839-4.

REFERENCES

Anderson, C. and Ratnieks, F. L. W. (1999). Worker allocation in social insect societies: coordination of nectar foragers and nectar receivers in honey bee (*Apis mellifera*) colonies. *Behav. Ecol. Sociobiol.* **46**, 73-81.

Biesmeijer, J. C., van Nieuwstadt, M. G. L., Lukács, S. and Sommeijer, M. J. (1998). The role of internal and external information in foraging decisions of *Melipona* workers (Hymenoptera: Meliponinae). *Behav. Ecol. Sociobiol.* **42**, 107-116.

Dreller, C. and Kirchner, W. H. (1993). Hearing in honeybees: localization of the auditory sense organ. *J. Comp. Physiol. A* **173**, 275-279.

Esch, H. (1961). Über die Schallerzeugung beim Werbetanz der Honigbiene. *Z. Vergl. Physiol.* **45**, 1-11.

Esch, H. (1967). Die Bedeutung der Lauterzeugung für die Verständigung der stachellosen Bienen. *Z. Vergl. Physiol.* **56**, 199-220.

Heinrich, B. (1993). *The Hot-blooded Insects: Strategies and Mechanisms of Thermoregulation*. Berlin, Heidelberg: Springer-Verlag.

Heran, H. (1959). Wahrnehmung und Regelung der Flugeigengeschwindigkeit bei *Apis mellifica* L. *Z. Vergl. Physiol.* **42**, 103-163.

Hrncir, M. (2003). Properties and significance of recruitment signals in a stingless bee (*Melipona seminigra* Friese 1903). PhD thesis, University of Vienna, Austria.

Hrncir, M., Jarau, S., Zucchi, R. and Barth, F. G. (2000). Recruitment behavior in stingless bees, *Melipona scutellaris* and *M. quadrifasciata*. II. Possible mechanisms of communication. *Apidologie* **31**, 93-113.

Hrncir, M., Jarau, S., Zucchi, R. and Barth, F. G. (2004a). Thorax vibrations in stingless bees (*Melipona seminigra*). I. No influence of visual flow. *J. Comp. Physiol. A* **190**, 539-548.

Hrncir, M., Jarau, S., Zucchi, R. and Barth, F. G. (2004b). Thorax vibrations in stingless bees (*Melipona seminigra*). II. Dependence on sugar concentration. *J. Comp. Physiol. A* **190**, 549-560.

Hrncir, M., Barth, F. G. and Tautz, J. (2006a). Vibratory and airborne sound-signals in bee communication. In *Insect Sounds and Communication: Physiology, Behaviour, Ecology, and Evolution* (ed. S. Drosopoulos and M. Claridge), pp. 421-436. Boca Raton, London, New York: CRC Press, Taylor & Francis Group.

Hrncir, M., Schmidt, V. M., Schorkopf, D. L. P., Jarau, S., Zucchi, R. and Barth, F. G. (2006b). Vibrating the food receivers: a direct way of signal transmission in stingless bees (*Melipona seminigra*). *J. Comp. Physiol. A* **192**, 879-887.

Hrncir, M., Gravel, A. I., Schorkopf, D. L. P., Schmidt, V. M., Zucchi, R. and Barth, F. G. (2008). Thoracic vibrations in stingless bees (*Melipona seminigra*): resonances of the thorax influence vibrations associated with flight but not those associated with sound production. *J. Exp. Biol.* **211**, 678-685.

Jacobsen, F., Poulsen, T., Rindel, J. H., Gade, A. C. and Ohlrich, M. (2007). *Fundamentals of Acoustics and Noise Control*. Ørsted: DTU, Technical University of Denmark.

King, M. J., Buchmann, S. L. and Spangler, H. (1996). Activity of asynchronous flight muscle from two bee families during sonication (buzzing). *J. Exp. Biol.* **199**, 2317-2321.

Lindauer, M. and Kerr, W. E. (1958). Die gegenseitige Verständigung bei den stachellosen Bienen. *Z. Vergl. Physiol.* **41**, 405-434.

Michelsen, A. (1993). The transfer of information in the dance language of honeybees: progress and problems. *J. Comp. Physiol. A* **173**, 135-141.

Michelsen, A. (2003). Signals and flexibility in the dance communication of honeybees. *J. Comp. Physiol. A* **189**, 165-174.

Michelsen, A., Kirchner, W. H. and Lindauer, M. (1986). Sound and vibrational signals in the dance language of the honeybee, *Apis mellifera*. *Behav. Ecol. Sociobiol.* **18**, 207-212.

Michelsen, A., Towne, W. F., Kirchner, W. H. and Kryger, P. (1987). The acoustic near field of a dancing honeybee. *J. Comp. Physiol. A* **161**, 633-643.

Morawetz, L. (2007). Reichweite und Übertragung vibratorischer Signale bei der Kommunikation stachelloser Bienen. Diploma thesis, University of Vienna, Austria.

Morawetz, L., Hrncir, M., Zucchi, R. and Barth, F. G. (2007). Propagation of vibrational signals in the nest structures of a stingless bee (*Melipona bicolor*). In *Proceedings of 10th Meeting Austrian Neuroscience Association*, Seggau, Austria, p. 26.

Morse, P. M. (1981). *Vibration and Sound* (4th edn). Woodbury, NY: American Institute of Physics of the Acoustical Society of America.

Nieh, J. C. (1998). The recruitment dance of the stingless bee, *Melipona panamica*. *Behav. Ecol. Sociobiol.* **43**, 133-145.

Nieh, J. C., Contrera, F. A. L., Rangel, J. and Imperatriz-Fonseca, V. L. (2003). Effect of food location and quality on recruitment sounds and success in two stingless bees, *Melipona mandacaia* and *Melipona bicolor*. *Behav. Ecol. Sociobiol.* **55**, 87-94.

Schneider, P. (1975). Versuche zur Erzeugung des Verteidigungstones bei Hummeln. *Zool. Jb. Physiol.* **79**, 111-127.

Snodgrass, R. E. (1956). *Anatomy of the Honey Bee*. Ithaca, NY: Cornell University Press.

Sokal, R. R. and Rohlf, F. J. (1995). *Biometry* (3rd edn). New York: Freeman.

Tsujiuchi, S., Sivan-Loukianova, E., Eberl, D. F., Kitagawa, Y. and Kadowaki, T. (2007). Dynamic range compression in the honey bee auditory system toward waggle dance sounds. *PLoS ONE* **2**, e234.

Wenner, A. M. (1962). Sound production during the waggle dance of the honeybee. *Anim. Behav.* **10**, 79-95.